JOURNAL OF Materials CHEMISTRY

The effects of radiation on the retention of strontium in zeolite-NaSrY

Binxi Gu, Lumin Wang and Rodney C. Ewing*

Department of Nuclear Engineering and Radiological Sciences, University of Michigan, Ann Arbor, MI 48109-2104, USA. E-mail: rodewing@umich.edu

Received 3rd August 2001, Accepted 7th November 2001
First published as an Advance Article on the web 7th January 2002

A new experimental method has been developed to measure the release of radionuclides from radiation-damaged materials using a combination of 500 keV H^+ beam irradiation, electron microscopy, and electron microprobe analysis techniques. A good correlation between the radiation damage and changes in the release of radionuclides from irradiated zeolite-Y preloaded with Sr has been established. After irradiation with a 500 keV H^+ beam to a dose of 3.6×10^{17} ions cm^{-2}, the release of Sr in 1 N NaCl, 1 N $CaCl_2$ and 10 mN $AgNO_3$ solutions was reduced by a factor of up to seven in the radiation-damaged material. A comparison of results obtained in 10 mN $AgNO_3$ solution with that of 1 N $CaCl_2$ solution showed that structural damage occurred not only to the supercages, but also to the small cages, *i.e.* sodalite cages and double 6-ring prisms. When the radiation dose was above 2.5×10^{10} Gy, the ion exchange of the large cations (Ca and Sr) was completely stopped, whereas the small cation-exchange (Ag and Na) could still proceed. A leach test in the deionized water showed that amorphization of zeolite-NaSrY can reduce the release of the adsorbed radionuclides, Sr, from 0.23 mg g^{-1} for crystalline zeolite-NaSrY to 0.12 mg g^{-1} after 234 h of leaching in 90 °C deionized water.

1 Introduction

Zeolites are of considerable interest in the nuclear industry because of their use as waste processing media, waste forms and potential back-fill materials in nuclear waste repositories.[1–6] Zeolite-group phases have also been identified as precipitates on the corroded surfaces of nuclear waste glasses.[7] Rare-earths, actinides, Cs, and Sr are retained in these alteration products through ion exchange reactions.[7,8] As the radiation dose received by the zeolite phases can be high (*ca.* 10^{10} Gy) after 100 years of storage of the waste forms in a nuclear waste repository,[9] radiation may cause structural damage in zeolites. The changes in the crystalline structure may in turn affect the physical and chemical properties (*e.g.* density, ion exchange and retention capacity) of zeolites. Radiation-induced defect structures and the crystalline-to-amorphous transformation of zeolites have been the subject of numerous studies over the past several decades.[10–14] A number of studies have shown that zeolites are relatively sensitive to electron beam damage. In addition to the crystalline-to-amorphous transformation, bubble formation and the changes in particle morphology have been observed during the course of radiation exposure.[10,11,14] Zeolites are also susceptible to other types of radiation such as gamma-, ion beam-, and neutron-irradiation.[15–17] Analcime and zeolite-5A were found to lose their long-range order at doses of 0.1 dpa (displacement per atom) and *ca.* 6×10^8 Gy with *ca.* 1–1.5 MeV krypton irradiation.[11,18,19] Structural damage in zeolite-A has been detected under neutron irradiation. Complete collapse of the crystalline structure occurred when the dose reached 7×10^{19} neutrons cm^{-2}.[16]

One of the most important properties of zeolites is their high cation exchange capacity, which forms the basis for the use of zeolites as an ion exchange medium for the radionuclides, such as caesium and strontium, rare-earths, and actinides, in the high-level liquid nuclear waste.[20] However, there are limited data on the effect of radiation on the release of the adsorbed radionuclides, due primarily to the difficulties in studying the chemical properties of the post-irradiated materials. In general, the standard tests used to investigate the chemical durability of waste forms are either not appropriate or are not sensitive enough to elucidate the effects of radiation damage on the elemental release process. Previous studies[16,17] have shown that the radiation-induced amorphization of zeolite can result in significant loss in the ion exchange capacity. Because the ion exchange reaction is a reversible process, the radiation-induced structural change may also effect the release of adsorbed radionuclides when the zeolite phases are in contact with aqueous solutions. As zeolites are to be used as waste forms or buffer materials in a nuclear waste repository for the containment of the radionuclides, the desorption behavior of the adsorbed radionuclides and the evolution of that behavior with increasing radiation dose are important in evaluating the long-term performance of a nuclear waste repository.

2 Experimental

2.1 Materials

Zeolite-NaY ($NaAlSi_2O_6 \cdot nH_2O$), was obtained from Zeolyst International Company in powder form. Sr-exchanged zeolite-NaY was prepared by ion exchange in 0.1 N $SrCl_2$ aqueous solution with a solid to solution ratio of 14 : 1000. The mixture was constantly agitated on a 150 rpm orbital shaker for 24 h at room temperature and then centrifuged at a speed of 3500 rpm for *ca.* 15–20 min. The supernatant solution was carefully decanted and the remaining solid phase was washed with deionized water and dried at 50 °C for 120 h. The Sr concentration in zeolite-NaSrY powder was *ca.* 12 wt.% (without accounting for structural water), as determined by Instrumental Neutron Activation Analysis (INAA). A portion of the dried zeolite-NaSrY powder was heated at 900 °C for 30 min followed by cooling in air. Complete amorphization of the thermally treated zeolite-NaSrY was confirmed by X-ray diffraction (XRD). Another portion of the zeolite-NaSrY powder was pressed at a pressure of *ca.* 18 MPa to form a 1.5 mm thick tablet, which was used in the subsequent H^+ beam irradiation. Based on the XRD analysis of the tablet

This journal is © The Royal Society of Chemistry 2002

samples, no structural damage was produced from the sample preparation. The density of the tablet (0.8 g cm^{-2}), as determined by geometrical measurements, was about 50% of the theoretical density.

2.2 Methods

2.2.1 H^+ beam irradiation. The zeolite-NaSrY tablet was irradiated with a 500 keV H^+ beam generated by a tandem ion accelerator at the University of Michigan Ion Beam Laboratory. The sample was irradiated with a scanned beam over an area of 6.25 cm^2 for 20 h with the current density maintained at 0.8 μA cm^{-2}. The corresponding dose rate was 5×10^{12} ions cm^{-2} s^{-1}. The cumulative dose was also measured using a Faraday cap, which yielded a total dose of 3.6×10^{17} ions cm^{-2}. A temperature of approximately 300 °C in the irradiated tablet was calculated as previously described in ref. 17.

2.2.2 Desorption. The desorption of Sr from H^+ irradiated zeolite-NaSrY was completed in 1 N NaCl, 1 N $CaCl_2$ or 10 mN $AgNO_3$ solution. A portion of irradiated zeolite-NaSrY sample (*ca.* 15 mg) was placed in a glass flask in contact with 25 ml solution at room temperature. The glass flask was changed with fresh solution every 4–6 h over a total desorption time of 25 h. At the end of the desorption reaction, the solid sample was rinsed using deionized water and dried at 50 °C for 72 h. Dried solid samples were analyzed for their cation-concentration using electron microprobe analyses (EMPA).

The desorption of Sr was also conducted for zeolite-NaSrY powders prior to and after thermal treatment at 900 °C. After pre-loading with Sr, or thermal treatment, the zeolite-Y powders were gently ground using a pestle and mortar to crush any aggregates formed during the drying or heating processes in order to ensure good dispersion of the particles in solution. A 40 mg powder sample was mixed with 30 ml of 1 N NaCl or 1 N $CaCl_2$ solution at room temperature. The mixtures were continuously agitated on an orbital shaker at 150 rpm. The solution was carefully removed every 4–6 h after centrifugation of the mixture at 3500 rpm, and the tube was then filled with fresh solution. After a total desorption time of 25 h, the powder was washed with deionized water and dried at 50 °C for 72 h and then analyzed for Sr concentration using INAA.

Leach tests of the crystalline and amorphous zeolite-NaSrY powders were performed in deionized water to compare the chemical stability of crystalline and amorphized zeolite-NaSrY in aqueous environments. Samples of 0.4 g zeolite-NaSrY, dispersed in *ca.* 10 g deionized water in Teflon® tubes, were placed in an oven at a temperature of 90 °C. After designated heating times (96, 162, 234 h), samples were centrifuged at 3500 rpm. The liquid phase was analyzed using inductively coupled plasma high resolution mass spectrometry (ICP-HRMS) for Sr, Na, Si and Al.

2.2.3 Chemical analysis by SEM EDS and EMPA. After the desorption reactions in NaCl, $CaCl_2$ or $AgNO_3$ solution, the irradiated zeolite-NaSrY samples were mounted in epoxy resin and polished for scanning electron microscopy (SEM) and electron microprobe analyses (EMPA). The sample surface was coated with a thin carbon film to avoid charge accumulation. SEM was performed using a Philips XL30 field emission gun scanning electron microscope operated at around 10–20 kV to examine the particle morphology over the cross-section of the irradiated samples. Chemical analysis with SEM was conducted through energy dispersive X-ray spectroscopy (EDS) in line scan mode. The elemental distributions on the cross-sections of the irradiated samples were measured for Sr, Ca, and Na. The cross-sectional samples were also analyzed with a Camaca CAMEBAX electron microprobe employing a wavelength dispersive system (WDS) to further quantify the change in the retention capacity as a result of irradiation. The Camaca PAP correction routine $\phi(\rho z)$, *i.e.* modified ZAF,[21] was used for data reduction. The chemical composition of Sr-exchanged zeolite-NaY was analyzed using a raster beam scanned over an area of 2.25 μm^2. The electron microprobe was operated at an accelerating voltage of 15 kV with a current of 10 nA.

3 Results and discussion

The zeolite-NaSrY, in its tablet form, was irradiated with a 500 keV H^+ beam to a total fluence of 3.6×10^{17} ions cm^{-2}. The variation of radiation dose along the depth of the target material was calculated using the computer simulation program SRIM 2000.[22] As shown in Fig. 1, the ionizing radiation dose is expressed in terms of electronic energy deposition (Gy) whereas the collisional effect is measured in terms of displacement per atom (dpa). The number of displaced atoms was calculated based on the assumption of a displacement energy of 25 eV for all the elements in the zeolite-NaSrY phase. The energy deposition increases progressively with increasing target depth, and reaches a maximum dose of *ca.* 3×10^{10} Gy at the depth of approximately 14 μm from the irradiated sample surface. A significant amount of damage was produced by ballistic collisions (>0.1 dpa), which occurs in a narrow band over the target depth of *ca.* 13–17 μm.

The irradiated zeolite-NaSrY has been examined using SEM, with the secondary electron (SE) image of the cross-section shown in Fig. 2. Contraction of the damaged zeolite particles is evidenced by the increase in the inter-particle pore size. The increase of the atomic density in the radiation-damaged zeolite particles has also been observed by Rees and Williams[16] using XRD and density measurements. Because zeolite is a microporous material that contains a large percentage of void space enclosed by different types of cages, the increase of atomic density implies that some or all of the cages in the zeolite collapsed upon radiation-induced amorphization. The width of the damaged region measured from the SEM image is in agreement with the proton range calculated using the SRIM program (Fig. 2). The sample shown in Fig. 2 was eluted with 1 N NaCl after H^+ beam irradiation, in order to investigate the change of radionuclide release with the extent of radiation damage. The qualitative compositional changes along the depth of irradiation samples were measured using energy dispersive X-ray spectroscopy (EDS) on an SEM. The EDS spectra taken from the damaged (frame A) and undamaged regions (frame B), as labeled in Fig. 2, are shown in Fig. 3. Based on the previous study of the H^+ beam irradiated zeolite-NaY,[17] no appreciable amount of silicon concentration change

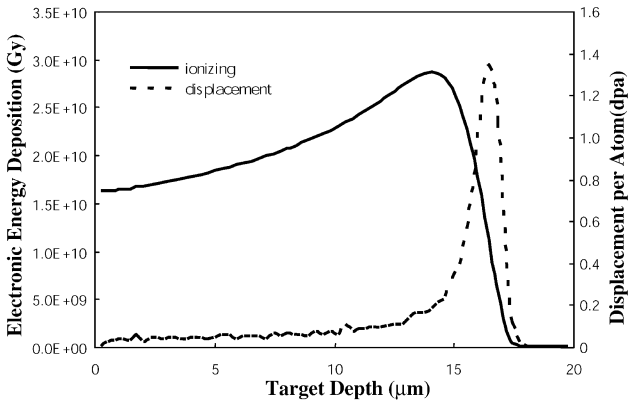

Fig. 1 Energy deposition and displacement production profiles along the depth of 500 keV proton penetration for zeolite-NaSrY with an irradiation dose of 4×10^{17} ions cm^{-2} (20 h) calculated using SRIM 2000.

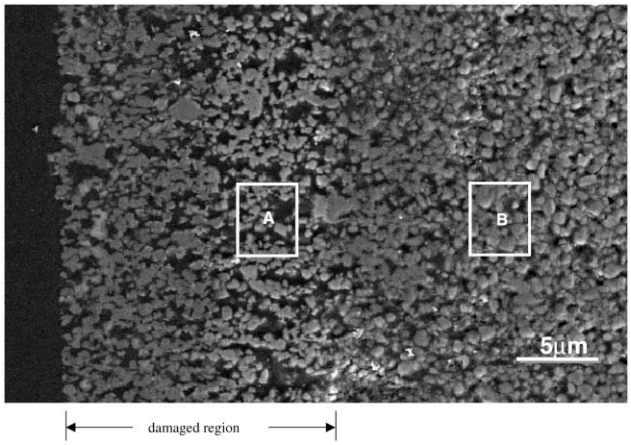

Fig. 2 SEM secondary electron image of the cross section of H^+ irradiated zeolite-NaSrY with a dose of 3.6×10^{17} ions cm^{-2}. The sample was used to conduct a desorption experiment in 1 N NaCl solution after irradiation.

occurs as a result of radiation damage followed by room temperature ion exchange. The spectra obtained from different locations of the sample in cross-section were, therefore, normalized according to the peak intensity of Si. The higher Sr peak intensity and lower Na peak intensity in the damaged region and the reverse correlation of Na and Sr peaks in the undamaged region indicate that the radiation damage in the crystalline structure may lead to a decrease in the desorption of Sr in the aqueous environment containing exchangeable cations. Desorption experiments of the irradiated zeolite-NaSrY were also conducted in 1 N $CaCl_2$ solution. The changes in the Sr- and Ca-concentration along the radiation-damaged region were measured using EDS in line scan mode. The changes in Sr- and Ca-concentration as a function of target depth from the irradiated surface are shown in Fig. 4. Lower Ca concentration and higher Sr concentration in the damaged region further confirmed the decrease of Sr desorption as a result of radiation damage.

Owing to the large error (up to 20%) in the EDS analysis, the result can only show the radiation effects on the retention capacity for the adsorbed radionuclides on a qualitative basis. The electron microprobe analysis was therefore used to obtain quantitative compositional data. Fig. 5 shows the change of Sr-, Ca- and Na-concentration as a function of depth in the zeolite-NaSrY sample irradiated by a 500 keV H^+ beam, followed by desorption in 1 N $CaCl_2$ solution. The Sr concentration increases with increasing sample depth. This corresponds to an increase of ionizing radiation dose as

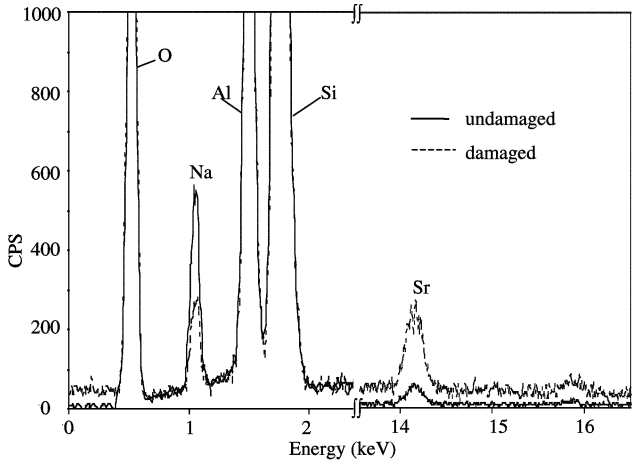

Fig. 3 SEM EDS spectra acquired from fully damaged region (Fig. 2, frame A.) and undamaged region (Fig. 2, frame B) of zeolite-NaSrY.

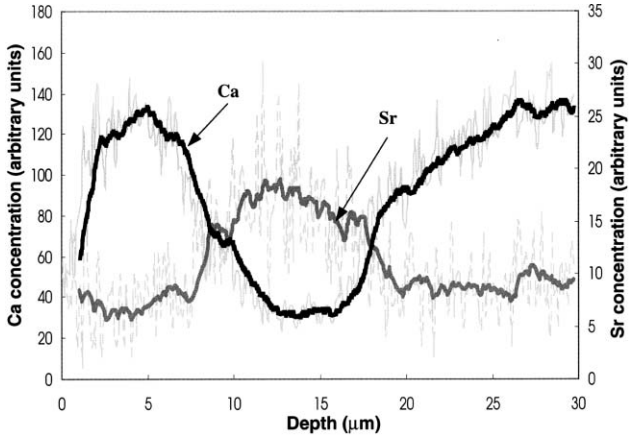

Fig. 4 EDS results on the Ca- and Sr-concentration along the cross-section of the H^+ beam irradiated zeolite-NaSrY followed by desorption in 1 N $CaCl_2$ solution. The concentrations are presented in arbitrary units. The dashed lines show the original data. The thick trendlines obtained from 10 periods moving-average of the original data show the compositional change more clearly.

determined by SRIM 2000 calculation (Fig. 1). The Sr concentration reaches a maximum of *ca.* 2.5 at.% at a depth of 8 μm, which corresponds to an ionizing radiation dose of 2×10^{10} Gy and a displacement damage of 0.05 dpa. According to the previous study of the structure of proton-damaged zeolite-NaY by transmission electron microscopy (TEM),[17] this dose can be related to the amorphization dose of zeolite-NaSrY resulting from ionizing radiation. The Sr concentration in the peak region is approximately 10 wt.%, indicating that more than 80% of Sr (as compared with the Sr concentration of 12 wt.% in zeolite-NaSrY before desorption experiments) is retained in the radiation-damaged zeolite-NaY. On the other hand, the Sr oncentration is only 1.5 wt.% in the undamaged region. The difference in the Sr concentration in the damaged and undamaged regions shows that radiation damage to the zeolite-NaSrY structure can result in a decrease in the release of adsorbed radionuclides by a factor of 7. The reduction of Sr desorption in the radiation-damaged region is further confirmed by the change in the Ca concentration as a function of depth. Ca concentration in the peak damage region (*ca.* 0.2 wt.%) is much lower than in the undamaged region (*ca.* 3 wt.%). A sudden increase in Na concentration from *ca.* 0.6 at.% in the undamaged region to *ca.* 1.5 at.% in the damaged region is yet to be understood. Based on the INAA analysis of the original zeolite-NaSrY, the ion exchange reaction between zeolite and Sr is incomplete even in the supercage. According to the structure of zeolite-NaY, about

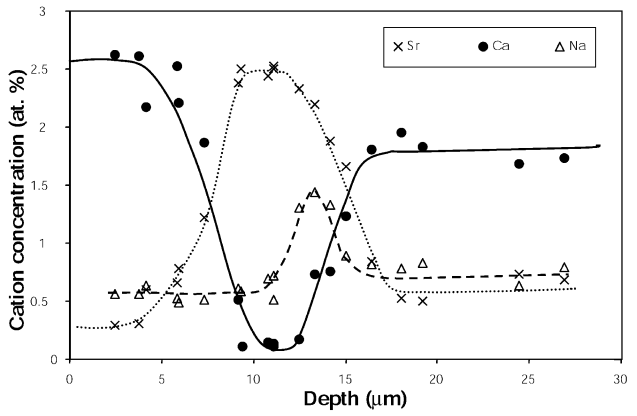

Fig. 5 Concentration profiles of exchangeable cations in the 500 keV H^+ irradiated zeolite-NaSrY with a dose of 3.6×10^{17} ions cm^{-2} followed by desorption in 1 N $CaCl_2$ solution. The results were obtained using EMPA.

68% of Na ions are located in the supercage.[23] INAA shows that only 60% of Na ions have been exchanged with Sr, and around 8% of Na ions in the supercage may still be exchanged by Ca. In the highly damaged region, the collapse of the supercages upon radiation exposure causes not only the fixation of large cations such as Sr, but this process may also trap smaller cations, such as Na, which makes Na no longer available for the exchange. However, we should also be aware that the compositional data obtained for Na using electron beam analysis may involve a large error due to the diffusion of Na under electron beam conditions.[24]

A similar Sr concentration profile has also been observed in the H^+ beam irradiated zeolite-NaSrY reacted with 1 N NaCl solution (Fig. 6). The Na concentration shows the opposite relation as compared with that of Sr. This result again confirmed that the radionuclides adsorbed on the zeolite might easily leach out when the undamaged waste form comes into contact with aqueous solutions containing exchangeable cations. Radiation damage to the structure can enhance the retention capacity of radionuclides in zeolite-NaSrY by a factor of 7.

One possible explanation for the reduction of Sr release in the radiation-damaged zeolite is associated with the collapse of cages, which makes the cations inside the cages inaccessible. There are three different types of cages in the zeolite-Y structure: supercages, sodalite cages (or the β cage), and double 6-ring prisms. A supercage is connected to four other supercages *via* a 12-ring window with a free aperture of 0.77 nm. The sodalite cages, which are connected to four adjoining supercages *via* 6-ring openings of 0.22 nm, are linked together by the double 6-ring prisms.[23] Exchangeable cations are located in all three types of cage. As observed in the previous study and by a number of other researchers,[10,17,25] the amorphization of zeolite is usually accompanied by distortion and shrinkage of the crystal. The relative sizes of the ions in solution and the apertures in the crystalline structure determine whether or not the ion exchange reaction can proceed. For Sr–zeolite-NaY ion exchange, the reaction can only occur in the supercage for which the aperture size is larger than the size of Sr ion ($d = 0.23$ nm). When the crystalline structure collapses, the aperture shrinks, and exchangeable cations are trapped inside the structure. Trapping of radionuclides in specific sites of a condensed Cs silicotitanate phase has been observed by Nyman *et al.*[26] However, the process of cage collapse is not fully understood. For example, we do not know whether the smaller cages collapse as well upon radiation damage to the crystalline structure. To further investigate the damage mechanism, a small and highly polarizable cation, Ag ($d = 0.25$ nm), was used in the desorption experiment after the zeolite-NaSrY was irradiated with 500 keV protons. Although slightly larger than the 6-ring aperture size (0.22 nm), Ag can still penetrate the aperture into the sodalite cages and the double 6-ring prisms, and this gives rise to a complete exchange with Na in these small cages. This is because the framework charge in zeolite-Y is sufficient to polarize the Ag ions enough to allow them to enter the small cages.[23]

The electron microprobe analysis results of the Sr-, Ag- and Na-concentration in the irradiated sample are presented in Fig. 7. By comparing Figs. 5, 6 and 7, we have noted that the shape and peak concentration of Sr are close for all three of the figures, suggesting that the radiation effects on the release of Sr are determined primarily by the property of Sr itself. The types of cations in the desorbent have little effect. This is understandable in terms of cage collapse mechanism. Based on the diameter of the Sr ion (0.23 nm), the exchange reaction can only occur in supercages at room temperature. Once the supercage collapses, the ion exchange capacity is determined primarily by large cations. Although the small cations in the solution may still be able to penetrate into the structure, the Sr trapped in the supercages cannot escape. This suggestion is further confirmed by the differences in the Ag and Ca concentration profiles. In the case of Sr–Ca reaction, the changes of Ca- and Sr-concentration along the target depth compensate each other. In the case of Ag, however, the amount of Ag adsorbed by zeolite is much higher than the amount of Sr released in both damaged and undamaged regions. Higher Ag concentration (*ca.* 6.5 at.%) than Ca concentration (1.8 at.%) as observed in the undamaged region is consistent with the results obtained by Sherry,[27] indicating that Ag^+ ions are small enough to penetrate the rings of six $(Si,Al)O_4$ tetrahedra and exchange with Na^+ in sodalite cages. Unlike the Ca concentration profile in Fig. 5 the bottom of the Ag-concentration profile is narrower with a higher trough concentration value (*ca.* 0.6 at.%) as compared with that of Ca (*ca.* 0.1 at.%). The decrease of Ag concentration with increasing radiation dose indicates that radiation damage may also cause damage to the smaller cages, which is responsible for the decrease of ion exchange capacity with Ag. However, this process requires a higher radiation dose, as is suggested by the concentration profile of Ag (Fig. 7). Even at the highest radiation dose achieved in this experiment (*ca.* 3×10^{10} Gy), some of the large and small cage apertures are still large enough to allow the penetration of Ag^+ and Na^+.

A common method of evaluating the long-term durability of the nuclear waste forms and other materials is to perform a

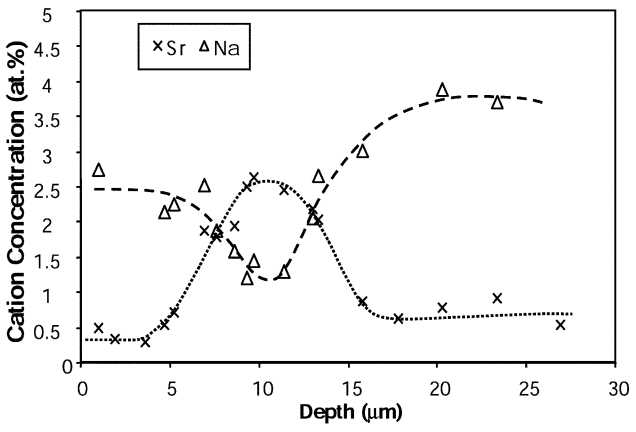

Fig. 6 Concentration profiles of exchangeable cations in the 500 keV H^+ irradiated zeolite-NaSrY with a dose of 3.6×10^{17} ions cm^{-2} followed by desorption in 1 N NaCl solution. The results were obtained using EMPA.

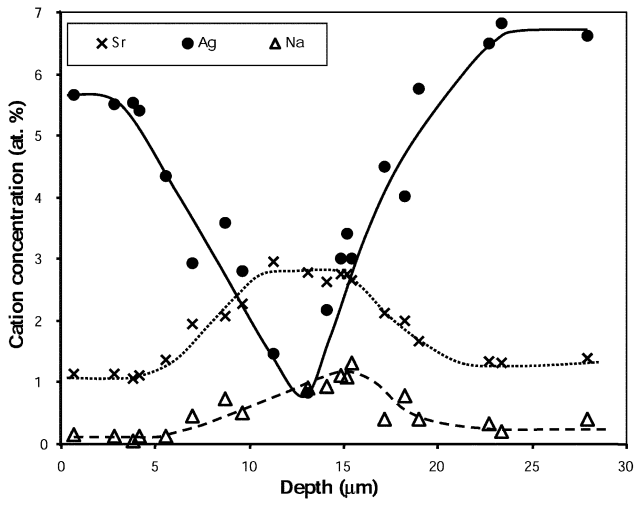

Fig. 7 Concentration profiles of exchangeable cations in the 500 keV H^+ irradiated zeolite-NaSrY with a dose of 3.6×10^{17} ions cm^{-2} followed by desorption in 10 mN $AgNO_3$ solution. The results were obtained using EMPA.

leach test following standard procedures. However, owing to the insensitivity of electron microprobe analysis to the small variation in the cation concentration resulting from the leaching experiments, this method cannot be used to determine the leach rate in deionized water. Previous studies have shown that the thermally- and radiation-induced amorphization can result in similar effects in the ion exchange capacity of the zeolite.[17] Thermally amorphized zeolite-NaSrY may, therefore, also provide valuable information on the chemical durability and damage mechanism of zeolites under irradiation. The zeolite-NaSrY thermally treated at 900 °C is completely amorphized as indicated by XRD. This sample was used for the leach test.

Table 1 compares the desorption of Sr from the original crystalline zeolite-NaSrY and thermally amorphized zeolite-NaSrY in 1 N NaCl or 1 N $CaCl_2$ solutions. The amorphous zeolite-NaSrY was obtained by heating the Sr-exchanged zeolite-NaY at 900 °C. The amount of Sr desorbed from the crystalline zeolite-NaSrY is approximately two orders of magnitude higher than that of the amorphous zeolite-NaSrY. The Sr concentrations in the crystalline zeolite-NaSrY are 0.39 and 0.45 wt.% after desorption in 1 N NaCl and 1 N $CaCl_2$ solutions, respectively. On the other hand, the Sr concentrations in the amorphous zeolite-NaSrY, after interaction with the same solutions of the same concentrations, are 12 and 11.3 wt.%, respectively. A comparison of the desorption in the thermally amorphized zeolite-NaSrY in NaCl, and $CaCl_2$ solutions (Table 1) with that of the radiation-damaged samples suggests that both processes do have a similar effect on the desorption behavior of the zeolites. The collapse of the cages during the thermal amorphization may result in the loss of ion exchange capacity due to the creation of inaccessible exchangeable sites.

Table 2 shows the desorption and/or leaching of cations from the original and thermally-amorphized zeolite-NaSrY in 90 °C deionized water. In the original crystalline zeolite-NaSrY, the release of Na is almost an order of magnitude higher (*ca.* 3.4–4.1 mg g^{-1} for leaching times of *ca.* 96–234 h) than in the thermally amorphized zeolite-NaSrY (*ca.* 0.46–0.61 mg g^{-1} over the same leaching times). The amount of Sr released from the crystalline zeolite-NaSrY phase is also higher as compared with the amount released from amorphized zeolite-NaSrY. The amount of Sr released into the solution varies from 0.15 to 0.23 mg g^{-1} for leaching times of 96 and 234 h, respectively. On the other hand, the release of Sr increases much more slowly with leaching time in the amorphized form. Over the same period of leaching, the Sr release changed from 0.11 to 0.12 mg g^{-1}. The reduced amount of the exchangeable cations released from the amorphized zeolite-NaSrY again confirms that the collapse of the zeolite structure can enhance the retention capability for radionuclides.

Both Al and Si are the framework-forming cations in the crystalline zeolite. However, the behaviors of these cations in the thermally amorphized zeolite-NaSrY are different. The leach rates for Al in the amorphized zeolite-NaSrY (*ca.* 0.3 mg g^{-1}) is an order of magnitude higher than in the crystalline zeolite-NaSrY (*ca.* 0.03 mg g^{-1}). This result suggests that chemical bond breakage may have occurred during the thermal process, which leads to a conversion of framework Al to non-framework Al. In contrast, the Si release rate after thermal treatment (*ca.* 0.6 mg g^{-1}) is slightly lower than that of unheated zeolite-NaSrY (*ca.* 0.7 mg g^{-1}). The change in the release rates of Si before and after thermal treatment (less than 20%) is much less than that for Al (an order of magnitude), suggesting that thermal amorphization may not have significant effects upon the Si tetrahedral network. Most of the Si remains in the framework structure after the crystalline-to-amorphous transition.

Table 2 The amount of cation desorbed from the unheated and thermally-amorphized (900 °C) zeolite-NaSrY in deionized water at 90 °C

		Amount of cation released/mg g^{-1}			
ID	Leaching time/h	Na	Al	Si	Sr
Unheated zeolite-NaSrY					
Z-Sr-1	96	3.41	0.033	0.69	0.15
Z-Sr-2	162	3.62	0.030	0.69	0.19
Z-Sr-3	234	4.10	0.023	0.71	0.23
900 °C treated zeolite-NaSrY					
Z-Sr-5	96	0.46	0.252	0.54	0.11
Z-Sr-6	162	0.51	0.230	0.52	0.11
Z-Sr-4	234	0.61	0.298	0.63	0.12

4 Conclusions

Radiation-induced structural damage in zeolite-NaSrY can result in significant changes in the release of Sr in NaCl, $CaCl_2$ and $AgNO_3$ solutions. The desorption of Sr is reduced due to the collapse of large cages in the zeolite structure, which helps to trap preloaded radionuclides, indicating that the structural damage in near-field materials may be beneficial for retarding the release of radionuclides from a geologic disposal repository into the biosphere. A comparison of results obtained in 10 mN $AgNO_3$ solution with that of experiments in 1 N $CaCl_2$ solution shows that structural damage occurs not only for the super-cages, but also for the small cages, *i.e.* sodalite cages and double 6-ring prisms. When the radiation dose is above 2.5×10^{10} Gy, the ion exchange of the large cations (Ca and Sr) is completely stopped, whereas the small cation exchange (for Ag and Na) can still proceed. Static leaching of crystalline and amorphous zeolite-NaSrY in the 90 °C deionized water samples shows that amorphization of zeolite-NaSrY can reduce the release of the adsorbed radionuclide, Sr, from 0.23 mg g^{-1} for crystalline zeolite-NaSrY to 0.12 mg g^{-1} after 234 h of leaching in 90 °C deionized water.

Acknowledgements

Authors thank Dr Victor Rotberg at the Michigan Ion Beam Laboratory for the assistance in proton irradiation experiments. The SEM and EMPA were conducted in the Electron Microbeam Analysis Laboratory at the University of Michigan. ICP Analyses were performed by Dr Ted Huston in the Keck Elemental Geochemistry Laboratory within the Department of Geological Sciences at the University of Michigan. This work was supported by the Department of

Table 1 Desorption data for Sr in different chemical solutions as determined from the powder zeolite-NaSrY samples using neutron activation analysis

Sample ID	Sample conditions	Solution composition	Reaction time/h	Sr concentration in solid (wt.%)
Z-Sr-7	Unheated zeolite-NaSrY	1 N NaCl	25	0.39
Z-Sr-8	900 °C heated zeolite-NaSrY	1 N NaCl	25	12.055
Z-Sr-9	Unheated zeolite-NaSrY	1 N $CaCl_2$	25	0.45
Z-Sr-10	900 °C heated zeolite-NaSrY	1 N $CaCl_2$	25	11.345

Energy's Environmental Management Science Program through grant DE-FG07-97ER45652.

References

1 D. C. Grant, A. K. Saha, D. K. Poletz and M. C. Skiba, *AIChE Symp. Ser.*, 1998, **84**, 13.
2 M. F. Simpson, F. L. Yapuncich and G. Moore, *Sorption of Waste Salt from the Electrometallurgical Spend Fuel Treatment Process into Zeolite Using a High Temperature V-Mixer*, Argonne National Laboratory Report ANL-NT-135, Argonne National Laboratory, Argonne, IL, 1999.
3 J. K. Reilly, P. J. Grant, G. J. Quinn, T. C. Runion and K. J. Hofstetter, *ASTM Special Technical Publication*, ASTM, Philadelphia, PA, USA, 1985, vol. 2, p. 1238.
4 *A Study of the Isolation System for Geologic Disposal of Radioactive Waste*, National Research Council, National Academy Press, Washington, DC, 1983.
5 P. K. Sinha and V. Krishnasamy, *J. Nucl. Sci. Technol.*, 1996, **33**, 333.
6 H. Mimura and T. Kanno, *J. Nucl. Sci. Technol.*, 1985, **22**, 284.
7 W. L. Gong, L. M. Wang, R. C. Ewing, E. Vernaz, J. K. Bates and W. L. Ebert, *J. Nucl. Mater.*, 1998, **254**, 249.
8 J. A. Fortner and J. K. Bates, *Mater. Res. Soc. Symp. Proc.*, 1996, **412**, 205.
9 R. C. Ewing, W. J. Weber and J. F. W. Clinard, *Prog. Nucl. Energy*, 1995, **2**, 63.
10 M. M. J. Treacy and J. M. Newsam, *Ultramicroscopy*, 1987, **23**, 411.
11 S. X. Wang, L. M. Wang and R. C. Ewing, *J. Nucl. Mater.*, 2000, **278**, 233.
12 L. A. Bursill, E. A. Lodge and J. M. Thomas, *Nature*, 1980, **286**, 111.
13 R. Csencsits and R. Gronsky, *Ultramicroscopy*, 1987, **23**, 421.
14 D. R. Acosta, G. Vazquez-polo, R. Garcia and V. M. Castano, *Radiat. Eff. Defects Solids*, 1993, **127**, 37.
15 E. A. Daniels and M. Puri, *Radiat. Phys. Chem. Isot.*, 1986, **27**, 225.
16 L. V. C. Rees and C. J. Williams, *Trans. Faraday Soc.*, 1965, **61**, 1481.
17 B. X. Gu, L. M. Wang, S. X. Wang, D. G. Zhao, V. H. Rotberg and R. C. Ewing, *J. Mater. Chem.*, 2000, **10**, 2610.
18 B. G. Storey and T. R. Allen, *Mater. Res. Soc. Symp. Proc.*, 1998, **481**, 413.
19 L. M. Wang, S. X. Wang and R. C. Ewing, *Proceedings of the 8th International Conference on High-Level Radioactive Waste Management*, American Nuclear Society, LaGrange Park, IL, 1998 p. 772.
20 H. S. Sherry, *Adv. Chem. Ser.*, 1971, **101**, 350.
21 G. F. Bastin, F. J. J. van Voo and H. J. M. Heijligers, *X-Ray Spectrom.*, 1984, **13**, 91.
22 J. F. Ziegler, http://www.research.ibm.com/ionbeams/SRIM.
23 D. W. Breck, *Zeolite Molecular Sieves–Structure, Chemistry and Use*, Krieger Publishing Company, Malabar, FL, 1984.
24 B. A. Pluijm, J. H. Lee and D. R. Peacor, *Clays Clay Miner.*, 1988, **36**, 498.
25 Y. Yokota, H. Hashimoto and T. Yamaguchi, *Ultramicroscopy*, 1994, **54**, 207.
26 M. D. Nyman, F. Bonhomme, T. M. Nenoff, D. Teter, R. S. Maxwell, B. X. Gu, L. M. Wang and R. C. Ewing, *Chem. Mater.*, 2000, **12**, 3449.
27 H. S. Sherry, *J. Phys. Chem.*, 1966, **70**, 1158.